atmosphere

MDPI

Article

Temporal Variation and Potential Sources of Water-Soluble Inorganic Ions in $PM_{2.5}$ in Two Sites of Mexico City

Fernando Millán-Vázquez [1], Rodolfo Sosa-Echevería [2], Ana Luisa Alarcón-Jiménez [2], José de Jesús Figueroa-Lara [1], Miguel Torres-Rodríguez [1], Brenda Liz Valle-Hernández [1] and Violeta Mugica-Álvarez [1,*]

[1] Basic Sciences Department, Universidad Autónoma Metropolitana Campus Azcapotzalco, Av. San Pablo No. 420 Col. Nueva el Rosario C.P., Alcaldía Azcapotzalco, Mexico City 02128, Mexico; al2203801934@azc.uam.mx (F.M.-V.); jjfl@azc.uam.mx (J.d.J.F.-L.); trm@azc.uam.mx (M.T.-R.); blvh@azc.uam.mx (B.L.V.-H.)

[2] Sección de Contaminación Ambiental, Instituto de Ciencias de la Atmósfera y Cambio Climático, Universidad Nacional Autónoma de México, México City 04510, Mexico; rodsosa@unam.mx (R.S.-E.); ana.alarcon@atmosfera.unam.mx (A.L.A.-J.)

* Correspondence: vma@azc.uam.mx

Abstract: This study presents the characterization and source apportionment of water-soluble inorganic ions (WSII), contained in particulate matter with an aerodynamic diameter equal to or less than 2.5 μm ($PM_{2.5}$), performed using the positive matrix factorization model (PMF). $PM_{2.5}$ were collected in Mexico City from two sites: at Merced (MER), which is a residential location with commercial activities, and at Metropolitan Autonomous University (UAM), which is located in an industrial area. The monitoring campaign was carried out across three seasons named Hot Dry (HD) (March–June), Rain (RA) (July–October), and Cold Dry (CD) (November-February). $PM_{2.5}$ concentration behavior in both sites was similar, following the order: CD > HD > RA. The UAM site exhibited higher concentrations of $PM_{2.5}$, of the five cations (Na^+, Mg^{2+}, Ca^{2+}, K^+ and NH_4^+), and of the four anions (Cl^-, SO_4^{2-}, NO_3^- and PO_4^{3-}) than MER, since the UAM site is surrounded by several industrial zones. $PM_{2.5}$ average concentrations for UAM and MER were 28.4 ± 11.2 and 20.7 ± 8.4 μg m^{-3}, respectively. The ratio of cation equivalent to anion equivalent (CE/AC) showed that aerosol pH is acidic, which was confirmed by direct pH measurements. The sulfur oxidation rate (SOR) was 20 times larger than the nitrogen oxidation rate (NOR). Additionally, SO_4^{2-} was the most abundant ion during the whole year, especially during the CD season with 5.13 ± 2.5 μg m^{-3} and 4.9 ± 3.6 μg m^{-3} for UAM and MER, respectively, when solar radiation displayed a high intensity. On the opposite side, the conversion of NO_2 to NO_3^-, respectively, was low. The air mass backward trajectories were modeled using the National Oceanic and Atmospheric Administration (NOAA-HYSPLIT), which allowed us to know that differences in the mass trajectories during the days with higher concentrations were due to an effect of air recirculation, which favored $PM_{2.5}$ accumulation and resuspension. On the other hand, on the days with less $PM_{2.5}$, good air dispersion was observed. The main sources identified with the PMF model were secondary aerosol, vehicular, industrial crustal, and biomass burning for UAM, while for MER they were vehicular, secondary aerosol, and crustal.

Keywords: $PM_{2.5}$; water-soluble inorganic ions; air quality; acidity; Hysplit; PMF

Citation: Millán-Vázquez, F.; Sosa-Echevería, R.; Alarcón-Jiménez, A.L.; Figueroa-Lara, J.d.J.; Torres-Rodríguez, M.; Valle-Hernández, B.L.; Mugica-Álvarez, V. Temporal Variation and Potential Sources of Water-Soluble Inorganic Ions in $PM_{2.5}$ in Two Sites of Mexico City. *Atmosphere* **2023**, *14*, 1585. https://doi.org/10.3390/atmos14101585

Academic Editor: Célia Alves

Received: 16 September 2023
Revised: 16 October 2023
Accepted: 16 October 2023
Published: 20 October 2023

1. Introduction

The megacity Mexico City presents high atmospheric pollutant concentrations affecting health and the environment, such as atmospheric aerosols, which have aroused interest because they have been related to significant damage to the environment, climate change, and the health of people exposed to breathing polluted air, since it is associated with millions of premature deaths [1]. The pollutants emitted into the atmosphere participate intensely in physics and chemistry processes like cloud formation and radiative balance.

Meteorological conditions such as precipitation, wind direction, and speed are essential for the dispersion and removal of pollutants [2,3]. As a consequence of economic growth, reflected in the growth of the mobile and industrial activities, $PM_{2.5}$ can be emitted from different sources [4–6]. In addition, Mexico City presents geographic and climatic problems that make their dispersion difficult [7]. According with the World Health Organization, $PM_{2.5}$ is considered the best indicator of the level of health risk from air pollution, due to its association with a high number of deaths and respiratory illness and cancers [8]; for that reason, the government has imposed a maximum permissible limit of $PM_{2.5}$ exposure which must not exceed 41 $\mu g\ m^{-3}$ in 24 h.

$PM_{2.5}$ composition includes organic and inorganic species, which must be identified to have a better understanding of their behavior in the ambient air. Among them, the water soluble inorganic ions (WSIIs), are of major interest since they are significant components of atmospheric aerosols, and precursors of acid rain and secondary aerosol formation [9,10]. Several studies have reported the presence of WSIIs in $PM_{2.5}$ such as NO_3^-, F^-, K^+, Ca^{2+}, Mg^{2+}, Na^+, SO_4^{2-}, NH_4^+, and PO_4^{3-}, and high concentrations in the air indicate a serious environmental and health problem [11,12]. Some WSIIs are known as tracers of some emission sources, for instance, K^+ is a biomass burning tracer [13]; Ca^{2+}, PO_4^{3-}, and Mg^{2+} are often associated with crustal, and Cl^- is associated with biomass burning and soil dust [14]. Ions are associated with chemically complex mixtures that depend on hygroscopic properties and are usually found in 20 to 50% in the $PM_{2.5}$ composition [15–17]. Acid rain formation is an important environmental damage process that involves the water dissolution of atmospheric SO_2 and NO_2, which are typically associated with emissions from industrial and mobile sources, to transform them into sulfuric acid (H_2SO_4) and nitric acid (HNO_3), causing damage to people, the environment, and structures; additionally, SO_2 and NO_2 are important precursors in the formation of secondary aerosols such as $(NH_4)_2SO_4$ and NH_4NO_3 [18,19].

WSII measurement and quantification are required to estimate their formation rate from SO_2 and NO_2, using the sulfur oxidation rate (SOR) and nitrogen oxidation rate (NOR) [20]. Moreover, the seasonal distribution of each WSII helps to determine the sources and chemical transformations generated in the atmosphere and the associated damage to human health [21]. Nevertheless, although many PM characterization and source reconciliation studies have been published, there are relatively few studies regarding WSI; in addition, most of them have been performed only in China. Models have been used to obtain better knowledge about pollutant species. On the one side, the HYSPLIT model has been applied to obtain the dispersion and trajectory of pollutants such as $PM_{2.5}$. This tool provides the relationship between the origin of the wind masses and the receptor site [22]. On the other side, receptor models like PMF are useful to determine the main sources of $PM_{2.5}$ and its WSII [23,24]. In this research, $PM_{2.5}$ were collected in two sites in Mexico City during one whole year in order to carry out a comprehensive WSII research project that identified and quantified the ions, determined the ratio of equivalent anions and cations to estimate the sulfur and nitrogen oxidation rates (SOR and NOR), the $PM_{2.5}$ acidity, WSII source contribution, as well as the identification of the path where the pollutants came from.

2. Materials and Methods

2.1. Sampling Sites

For this study, two locations in Mexico City were selected (Figure 1). The first place was a building located at the Metropolitan Autonomous University Azcapotzalco (UAM), (19°30′13.6″ N 99°11′09.0″ W) 15 m above ground level; in this site, there are industrial activities that are carried out in the surroundings. The second site was La Merced (MER), a commercial and residential area in the downtown, where the equipment was installed on the high school building "Francisco Zarco", about 14 m above ground level; this site is part of the Automatic Atmospheric Monitoring Network (RAMA), which is in charge of measuring air quality in different areas of Mexico City. $PM_{2.5}$ aerosols were collected

every 6 days for 24 h, from December 2021 to December 2022. The monitoring campaign was carried out in three seasons, cold-dry (CD) from November 2021 to February 2022, hot-dry (HD) from March to June 2022, and rain (RA) from July to November 2022, with two Tish Environmental High-Vol model TE 5007. Pre-calcinated quartz fiber filters (Whatmann), 20 cm × 25 cm were used. Meanwhile, the concentrations of NO_2 and SO_2 and meteorological information were monitored and obtained by RAMA.

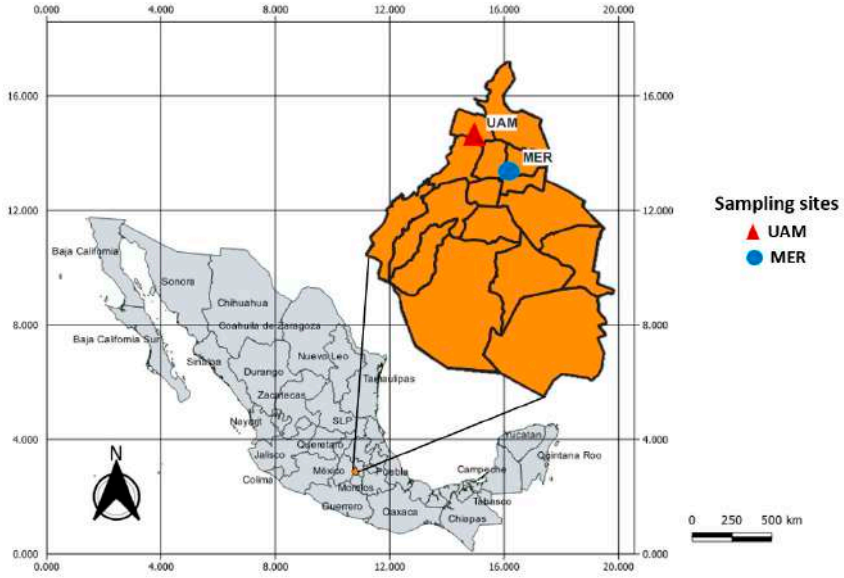

Figure 1. Sampling sites in Mexico City. Metropolitan Autonomous University (UAM), Merced (MER).

2.2. Identification and Quantification of Water Soluble Inorganic Ions

The quartz filters were cut for different analyses. An area of 2.05 cm^2 was selected for the ion measurements. Samples were extracted in 15 mL of ultrapure water with a resistivity of 18.2 MΩ*cm at 25 °C. All materials and high-density polyethylene bottles were cleaned with the same type of water. Ions were extracted via ultrasonic for 60 min < 35 °C and 37 Hz, followed by agitation (120 cycles) for 60 min and refrigeration for 12 h before reading. The aqueous extracts were analyzed by Ion Chromatography Metrohm 850 Professional (IC), with Metrosep C 4-100/4.0 and Metrosep A sup 7-250/4.0 ion exchange columns for cations and anions. Ion separation is based on their affinities for active sites; for anions, the analytical sample time was 39 min at a flow of 0.600 mL/min and a pressure of 16.01 MPa, whereas for cations, the analytical sample time was 15 min at a flow of 0.800 L/min and a pressure of 6.84 MPa.

2.3. Measurement of pH and Conductivity

Once the ions were measured via chromatography, a part of the aqueous extract was used for the pH determination using a Metrohm 916 Ti-Touch equipped with an electrode (pH 1–11). The equipment was calibrated with three buffer solutions with pH 4, 7, and 9 covering the entire range of samples. The conductivity for every sample was measured with a conductance meter YSI model 32 at 25 °C, and the equipment was calibrated with a Nist traceable standard solution TDS/Conductivity 442-15 (23.8 μs cm^{-1} at 25 °C).

2.4. Ion Balance and $PM_{2.5}$ Acidity

The cation equivalent to anion equivalent ratio in moles (CE/AE) has been used as an indicator to reflect the $PM_{2.5}$ potential acidity. Although it is only an empirical approach that strongly depends on the selection of ion species, it has been applied by many researchers

who have considered the same ions identified in this study [25–27]. Anion equivalents (AE) and cation equivalents (CE) were calculated using the following equations:

$$CE = \frac{[Na^+]}{23} + \frac{(NH_4^+)}{18} + \frac{([K^+])}{39} + \frac{([Mg^{2+}])}{12} + \frac{([Ca^{2+}])}{20} \quad (1)$$

$$AE = \frac{\left[SO_4^{2-}\right]}{48} + \frac{([NO_3^-])}{62} + \frac{([Cl^-])}{35.5} + \frac{([F^-])}{19} \quad (2)$$

where $[Na^+]$, $[NH_4{}^+]$, $[K^+]$, $[Mg^{2+}]$, $[Ca^{2+}]$, $[SO_4{}^{2-}]$, $[NO_3{}^-]$, $[F^-]$, and $[Cl^-]$ are the water soluble inorganic ion concentrations (nmol m^{-3}), and AE and CE are the anion and cation equivalents (nmol m^{-3}). If the CE/AE ratio is bigger than 1, $PM_{2.5}$ is alkaline; otherwise if it is less than 1, $PM_{2.5}$ is acidic [28]. Although F^- was measured in all samples, the concentrations were below detection limits. Other ions like $NO_2{}^-$, Br^-, and Li^+ were not measured due to their reported low concentrations in aerosol samples [29].

2.5. Conversion Flow Rate SOR and NOR

The conversion rate for NO_2 and SO_2 pollutants to secondary ions is estimated through the Sulfur Oxidation Rate (SOR) and Nitrogen Oxidation Rate (NOR) following the next equations [30]:

$$NOR = \frac{\left[NO_3^-\right]}{\left[NO_3^-\right] + [NO_2]} \quad (3)$$

$$SOR = \frac{\left[SO_4^{2-}\right]}{\left[SO_4^{2-}\right] + [SO_2]} \quad (4)$$

where $[NO_3{}^-]$ and $[SO_4{}^{2-}]$ are the ion molar concentrations, respectively, and NO_2 and SO_2 represent the airborne gas concentrations that were obtained from the automatic atmospheric monitoring network in the MER and CAM stations.

2.6. Aerosol Trajectories with HYSPLIT

An efficient tool to know the back trajectory of $PM_{2.5}$ air mass is the Hybrid Single Particle Lagrangian Integrated Trajectory Model (HYSPLIT); this model needs variables such as wind speed and direction [31–33]. The model domain was considered at 2000 m above ground level (AGL) and receptor back trajectories were simulated to 20 m AGL for both sites. These simulations were for 24 h; the two receptor locations were the initiation sites, where backwards trajectories were performed and generated every hour to obtain 6 trajectories every 4 h. Hysplit outputs were post-processed with Mathlab and Arcmap in order to visualize all the outputs simultaneously; instead, only one output was shown for the Hysplit model.

2.7. Receptor Model Analysis PMF

Positive matrix factorization has been used to determine the relationship between the receptor and sources [34,35]. Two data files are required as input data to the model: the concentration data, and their associated uncertainty. The PMF was used for the specific data matrix X of I by j dimensions. In addition, i means number of samples and j speciation species with its associated uncertainties u. Prior knowledge of the type and number of sources is not necessary for the use of the PMF model [36]. The model objective is solving Equation (3) where p means the number of factors and species f of every source.

$$X_{ij} = \sum_{k=1}^{p} g_{ik} f_{kj} + e_{ij} \quad (5)$$

The value e_{ij} means the residual element-related sample and species. This multivariance factor analysis transforms a matrix of speciated samples in two ways, G factor contributions and F factor profiles. And the model seeks to minimize the function Q in Equation (4), where U_{ij} is related to the uncertainty species.

$$Q = \sum_{i=1}^{m} \sum_{j=1}^{n} \left[\frac{X_{ij} - \sum_{k=1}^{p} g_{ik} f_{ij}}{U_{ij}} \right]^2 \quad (6)$$

The apportionment performed with positive matrix factorization (PMF) has been used as a tool for source identification. The diagnostic ratios can provide the identification of each source using $PM_{2.5}$ particle characterization and by finding the best solution, with the information based on the factor profiles of $PM_{2.5}$ concentrations, ions, and NO_2 and SO_2 data from a number of samples (n = 60); this USEPA tool identifies the main associated sources (profile factors) and their contributions [37,38].

2.8. Quality Control and Quality Assurance

Hi-Vols were calibrated for each new season. All plastic bottles were cleaned more than four times using deionized water until the measured conductivity was <0.8 µs cm^{-1} to 25 °C. In order to eliminate all organic impurities, quartz filters were pre-calcinated at 600 °C and put to a constant weight at a relative humidity of 35 ± 5% and temperature of 20 ± 5 °C. Field blank samples were included with the same extraction treatment and were subtracted from the samples. The internal standard was added every 10 samples. The Method Detection Limit (MDL) was predefined for quality control: 0.02, 0.08, 0.11, 0.11, 0.02, 0.02, 0.02, 0.01, and 0.04 mg/L for F^-, Cl^-, $SO_4{}^{2-}$, $NO_3{}^-$, Na^+, $NH_4{}^+$, K^+, Mg^{2+}, and Ca^{2+}, respectively. Data validation and ionic balance were carried out with the determined species, and a comparison between the measured and the calculated conductivity was made [39].

2.9. Statistical Analysis

A Shapiro–Wilk test was applied to the data of each site, finding that the data had no normality behavior; then, Mann–Whitney U tests were applied to make comparisons between sites and seasons for each species ($p < 0.05$), using Tibco Statistica 14—Ultimate Academic Bundle 32/64-bit (Perpetual License, Czech) software.

3. Results and Discussion

3.1. $PM_{2.5}$ and Water Soluble Inorganic Ion Concentrations

The annual mean $PM_{2.5}$ concentrations in UAM and MER were 28.4 ± 11.12 µg m^{-3} and 20.7 ± 8.4 µg m^{-3}, respectively. These values are much higher than the annual limit proposed by the WHO guidelines (5 µg m^{-3}), and exceeded, by a factor of 2.8 and 2.07, respectively, the Mexican national standard stated in the NOM-025-SSA1-2021 (10 µg m^{-3}). UAM annual median concentrations were 1.5 times larger than in MER, presenting significant differences, due to the industrial emissions in the surroundings. The median $PM_{2.5}$ concentrations are shown in Figure 2. The greatest $PM_{2.5}$ concentrations were found in the CD season, especially in December, due to the cold weather, atmospheric stability, and human activities, while the lowest were in the RA season during September, which is associated with atmospheric conditions like washing by rain precipitation occurring in this season. Additionally, moisture plays an important role in the growth of aerosol particles, $PM_{2.5}$ formation, and deposition. For the same reason, concentrations by season presented significant differences among RA compared with HD and CD in the UAM site, whereas in the MER, significant differences were found among the three seasons. Seasonal abundance concentrations were CD > HD > RA, in UAM, while in MER, the order was CD > RA > HD; this is because during the rainy season in MER, there was a work construction near the sampling site that increased the fine particle concentrations. Seasons CD and HD showed significant differences ($p < 0.05$) between UAM and MER. The correlation between UAM

and MER concentrations was small (R^2 = 0.48), suggesting different source contributions, as well as different meteorological conditions.

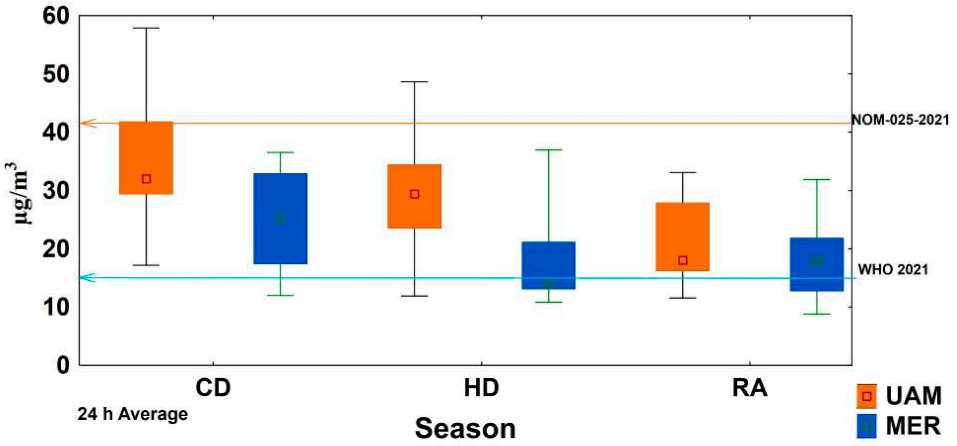

Figure 2. $PM_{2.5}$ concentration per season in Mexico City: (CD) Cold Dry, (HD) Hot Dry, (RA) Rain. (□ median value; horizontal lines in the box are the 25 and 75% percentiles, respectively; the bottom and top whiskers are the 5 and 95% percentiles, respectively. Red and blue lines are Mexican $PM_{2.5}$ standard and WHO guidelines).

Figure 3 presents the precursor gases serial times of SO_4^{2-} and NO_3^- in the two sites. NO_2 concentrations are around 1.6 times higher than SO_2, and it can be noted that trends have some differences, which are due to meteorological conditions and sources. SO_2 and NO_2 had higher concentrations in UAM because this site is near several industrial areas and there is high vehicular activity which impacts the air quality.

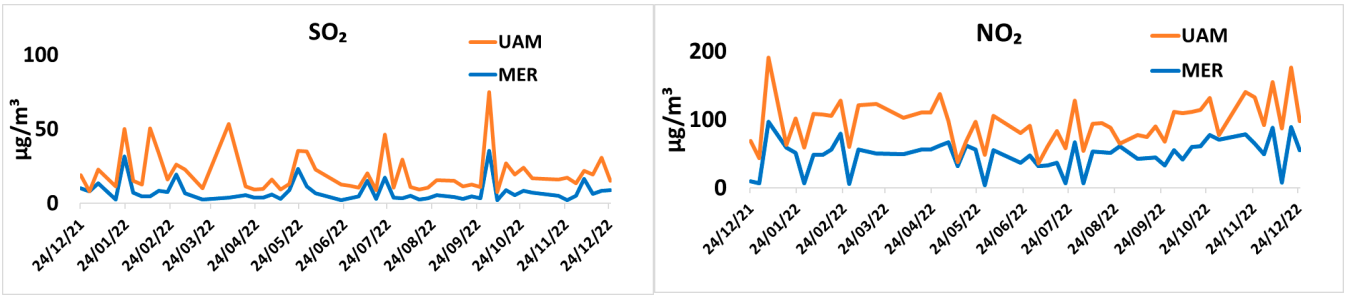

Figure 3. Serial times of secondary aerosol precursor gases.

The trends of major ions have some similarities in each location, suggesting similar sources in the surroundings; nevertheless, important differences can be appreciated between the two sites, indicating that ion sources or their contributions are not the same (Figure 4). Higher concentrations in UAM are also due to the nearby industrial facilities.

Table 1 displays the WSII and $PM_{2.5}$ concentration basic statistics. The three ions, known as SNA, presented the following abundance order, $SO_4^{2-} > NO_3^- > NH_4^+$, contributing from 50% to 70% of the total ions. Cl^- and alkaline ions K^+ and Mg^{2+} presented the lowest contributions. The WSII annual average concentrations were 10.9 ± 1.7 µg m^{-3} in UAM and in MER they were 10.07 ± 1.6 µg m^{-3}. The highest sum of ion concentrations was in the CD season with 12.7 ±1.7 µg m^{-3} and 11.9 ± 1.5 µg m^{-3} in UAM and MER, respectively; meanwhile, in the HD season, the WSII sums were 10.5 ± 1.5 µg m^{-3} and 8.7 ± 1.1 µg m^{-3} for UAM and MER, respectively. However, in the RA season, the WSII sum was slightly greater in MER than in UAM due to the construction works mentioned above.

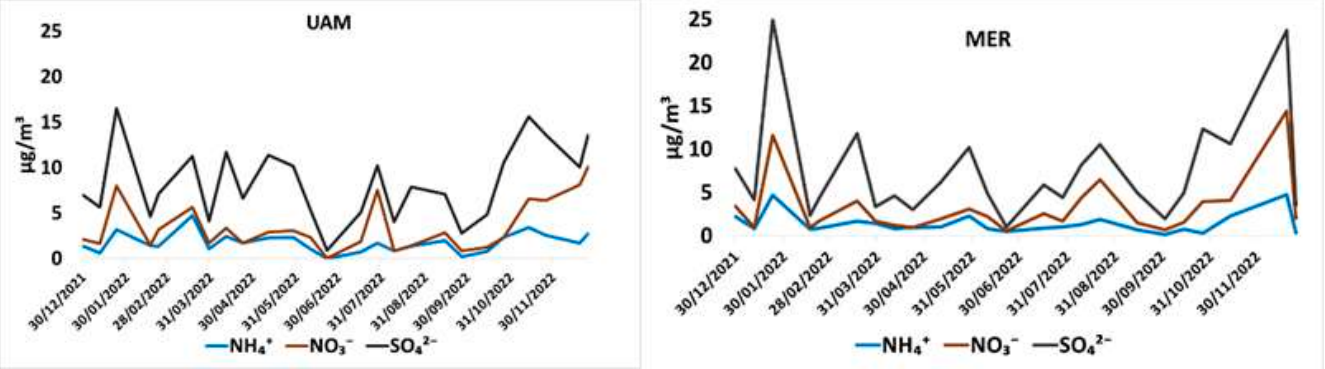

Figure 4. Serial times of major ions SO_4^{2-}, NO_3^-, and NH_4^+ (SNA) in UAM and MER.

Table 1. Descriptive Statistic of $PM_{2.5}$, gases, and water-soluble inorganic ions (µg m^{-3}).

SITE/SPECIES	N *	Mean	Median	Min	Max	SD	VC
UAM							
$PM_{2.5}$	61	28.4	28.5	11.2	62.3	11.2	39.4
SO_2	54	12.7	8.8	3.9	49.6	9.9	78.1
NO_2	55	46.4	48.3	3.8	93.9	20.5	44.2
Cl^-	23	0.1	0.1	0.0	0.1	0.0	45.5
SO_4^{2-}	25	4.8	4.0	0.9	9.0	2.4	50.6
Na^+	25	0.8	0.8	0.4	1.1	0.2	29.1
Mg^{2+}	25	0.1	0.1	0.0	0.2	0.0	63.3
Ca^{2+}	25	0.9	0.7	0.0	2.8	0.7	76.5
NO_3^-	25	1.7	0.8	0.0	7.4	2.2	125.8
K^+	21	0.2	0.2	0.0	0.4	0.1	61.8
NH_4^+	25	1.8	1.7	0.0	4.7	1.1	61.4
PO_4^{3-}	23	0.9	0.9	0.0	2.0	0.5	58.4
MER							
$PM_{2.5}$	61	20.7	18.8	8.8	41.1	8.4	40.4
SO_2	54	7.8	5.5	2.1	35.2	6.8	87.1
NO_2	57	46.1	51.5	3.4	97.1	24.0	52.1
Cl^-	23	0.1	0.1	0.0	1.9	0.4	263.6
SO_4^{2-}	24	4.3	3.4	0.5	13.4	3.0	71.4
Na^+	23	0.9	0.8	0.5	1.4	0.3	31.4
Mg^{2+}	24	0.1	0.1	0.0	0.2	0.0	62.9
Ca^{2+}	24	0.5	0.3	0.0	3.1	0.7	141.6
NO_3^-	24	1.9	0.9	0.0	9.7	2.3	126.3
K^+	24	0.2	0.1	0.0	2.6	0.5	240.6
NH_4^+	24	1.4	0.9	0.1	4.8	1.2	85.4
PO_4^{3-}	23	1.3	1.4	0.0	2.2	0.6	47.8

N * number of samples. SD standard deviation; VC variation coefficient.

3.2. Ion Balance and Seasonal Acidity

The ionic balance applied to verify the WSII measurements' validity is presented in Figure 5 for each site, exhibiting high determination coefficients (R^2) between $PM_{2.5}$ cations and anions (µeq L^{-1}): UAM: $R^2 = 0.81$ (a) and MER: $R^2 = 0.90$ (b). The correlation between the measured ions and conductivity (c) yielded a good correlation ($R^2 = 0.92$), meaning good ion chromatography measurements. The annual averages of $PM_{2.5}$ conductivities in UAM and MER were 14.6 ± 0.9 µs cm^{-1} and 10.4 ± 2.2 µs cm^{-1}, respectively, showing lower ion concentrations in the second site as well, as the ion measurements exhibited.

Figure 6 presents the UAM and MER CE/AE ratios from all of the samples. In all cases, ratios were slightly lower than one, suggesting $PM_{2.5}$ have a weak acidic or neutral behavior, and indicating the deficiency of cations to neutralize anions. It has also been indicated that some organic acid anions could be adsorbed in the aerosol [26,40]. The

seasonal ratio variation in UAM was HD > CD > RA with average values of 0.9, 0.85, and 0.8, respectively, while in MER, the seasonal ratio variation was CD > HD > RA with average values of 0.97 (practically neutral), 0.9, and 0.8. The pH values measured in UAM were 6.29, 6.03, and 6.06 in the HD, CD, and RA seasons, respectively, while in MER, the values were 6.27, 5.79, and 5.92 for the same seasons, confirming the $PM_{2.5}$ acid character determined using the ions. These results are in agreement with those of Guo et al. [41] and Geng et al. [42] but are opposite to those of Yin et al. [26] who presented values greater than one, probably due to the excess of alkaline ions.

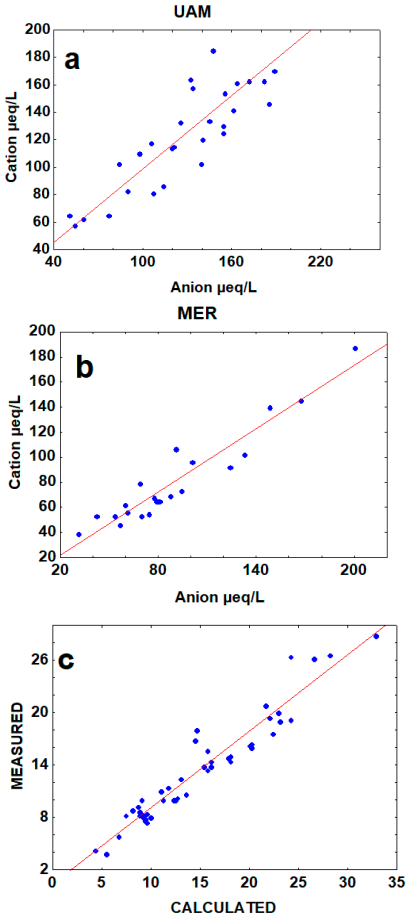

Figure 5. $PM_{2.5}$ cation and anion ratio in Mexico City, (**a**) UAM, (**b**) MER, (**c**) total measured/calculated conductivity.

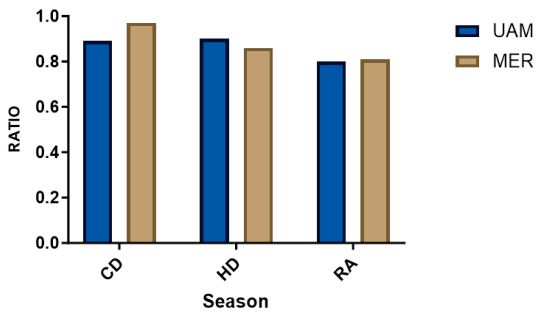

Figure 6. Anion–cation ratio in $PM_{2.5}$ in Mexico City.

3.3. Water Soluble Ion Concentrations

Ion concentrations accounted for 39.6 ± 5.7% and 49.5 ± 3.9% of $PM_{2.5}$ mass in UAM and MER, respectively, presenting significant differences. The rest of the PM mass was

composed of carbonaceous and silica materials not assessed in this work. WSII percentages are shown in Figure 7 by site and season. The most abundant ion was by far the SO_4^{2-}, with more than 40% of the WSII mass, followed by NH_4^+ and NO_3^- in both sites, which is in accordance with reported studies in other countries [43,44]. The high SO_4^{2-} contribution indicates direct gas emissions followed by atmospheric reactions and secondary aerosol formation [45].

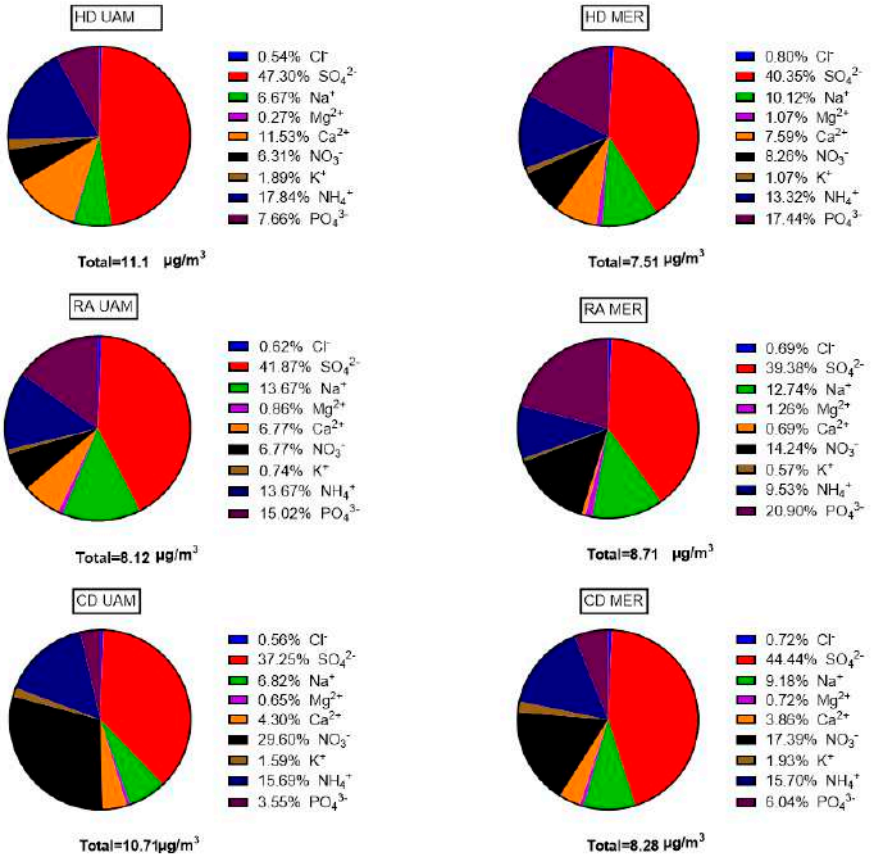

Figure 7. Percentages of individual ions to the total WSII mass. It is possible to observe that contributions to the WSII are not the same in the sites nor in the different seasons because the source contributions can be different, the weather varies, as well as the speed and wind direction. The lower K^+ concentrations were during the rainy season; this can be explained because this ion is a biomass-burning tracer, and, in that season, there were no wildfires.

3.4. Water Soluble Inorganic Ion Concentrations

Figures 8 and 9 show the most and least abundant WSII concentrations. Although the most abundant anions and cations (SNA), SO_4^{2-}, NO_3^-, and NH_4^+, had higher concentrations in UAM than in MER, they did not present significant statistical differences in the annual averages, although there were some differences between seasons. NH_4^+ presented its highest concentration in the HD season with 1.98 ± 1.4 µg m^{-3} in UAM, but there were no statistically significant differences.

With the exception of Ca^{2+} and PO_4^{3-} which had higher annual average concentrations in MER than in UAM with statistically significant differences, the other ions with less abundant concentrations had no differences; the reason for that may be due to the construction work close to the MER site that took several months and increased the Ca^{2+} and PO_4^{3-} emissions; moreover, these ions presented some significant differences among different seasons, since the main source is crustal.

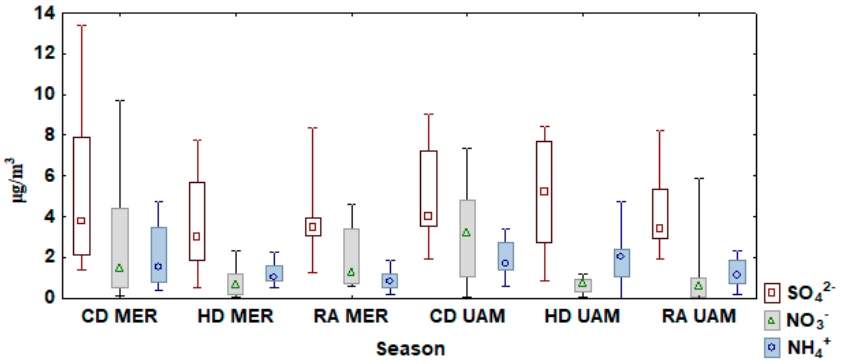

Figure 8. Most abundant WSII in $PM_{2.5.}$ (□ median value; horizontal lines in the boxes are the 25 and 75% percentiles, respectively; and the bottom and the top whiskers are the 5 and 95% percentiles, respectively).

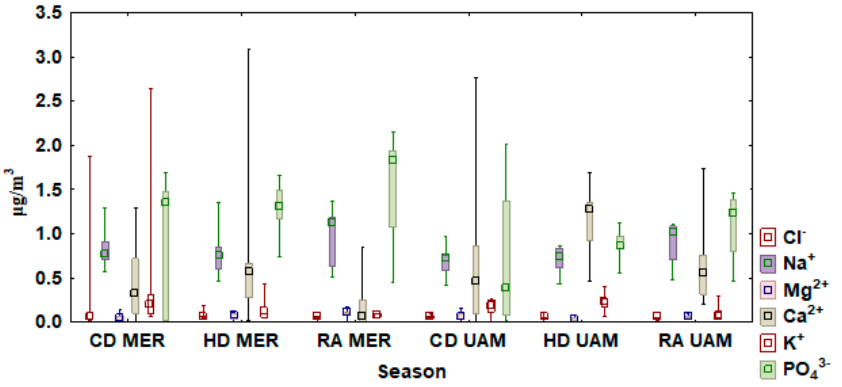

Figure 9. Less abundant WSII in $PM_{2.5}$. (□ median value; horizontal lines in the boxes are the 25 and 75% percentiles, respectively; and the bottom and the top whiskers are the 5 and 95% percentiles, respectively).

3.5. Sulfur Oxidation Rate and Nitrogen Oxidation Rate

The annual averages of NOR and SOR, related to the atmospheric conversion of SO_2 and NO_2 into secondary aerosols, are shown in Figure 10. In both sites, SOR was up 5 to 20 times larger than NOR which is consistent with other studies [26,46]. The SOR annual median was 0.21 ± 0.06 and the three seasons and sites had similar SOR results, ranging between 0.21 and 3.4. These values indicate that sulfate secondary aerosol production was high, since SO_2 photochemical oxidation to SO_4^{2-} takes place when SOR is greater than 0.1 [46,47]. Other authors have reported the lowest SOR values during winter, due to it being the season when solar radiation decreases, and this condition does not favor the SO_2 oxidation that involves also the OH^- radical with further condensation and sorption into the $PM_{2.5}$ [26]. Nevertheless, in Mexico City, the UV radiation intensity is very high (11–15, on the WHO scale) from the beginning of February to the end of October, but it is high (7–10 on the WHO scale) during the other months. Then, the SO_2 photochemical oxidation is favored the whole year, maybe due to the saturation of the gas–ion transformation.

The NOR annual median was 0.015 ± 0.01, with higher values during the CD and the RA seasons in UAM and MER respectively, ranging from 0.01 to 0.06 with no significant differences between the sites; these small values indicate that the secondary transformation of NO_2 was low since NOR is much lower than 0.1 and that NO_3^- comes mainly from primary source emissions [46]. In Mexico City, NO_2 emissions are produced primarily by vehicles, industries, and the power plants located to the north of the city, and both sites have important avenues close to the monitoring stations. The lowest NOR values were observed during the HD seasons, with values up to six times smaller, because this season's experiments took place under high temperatures. Additionally, the secondary

aerosol formed (NH_4NO_3), which can be evaporated and discomposed into its precursor gases SO_2 and HNO_3; this behavior has been described in other works where higher NOR values are observed in cold seasons in comparison with spring and summer [26,48].

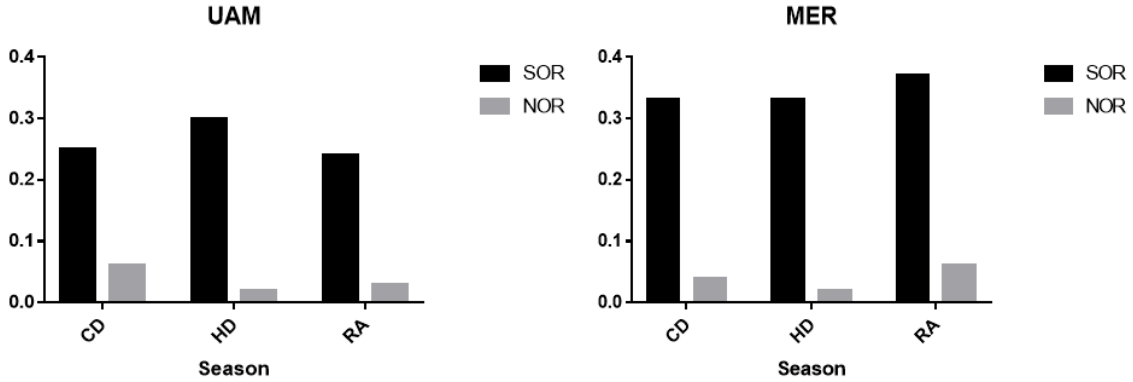

Figure 10. Variations in NOR and SOR in UAM and MER during different seasons.

3.6. Molar Ratios

MER presented a higher correlation between molar concentrations of SO_4^{2-} and NH_4^+ ($R^2 = 0.7$) than in UAM ($R^2 = 0.53$), whereas correlations between NH_4^+ and NO_3^- were lower in both sites: MER with $R^2 = 0.49$ and UAM with $R^2 = 0.18$. These results suggest that in MER, the anthropogenic emission sources of those three ions have higher similarities than in UAM. Figure 11 illustrates the relationships between the average ions of both sites. The relationship between NH_4^+ and the sum of the two cations indicates the neutralization of sulfate and nitrate by the ammonium. The low concentration of NH_4NO_3 may be due to it having a higher vapor pressure than $(NH_4)_2SO_4$; then, this last compound is formed before NH_4NO_3. Moreover, when NH_4^+/SO_4^{2-} is > 2, the aerosol is ammonium rich, but in the two sites in Mexico City, this ratio is <1 meaning it is ammonium-poor, and NH_4NO_3 is maybe more related to crustal species [46].

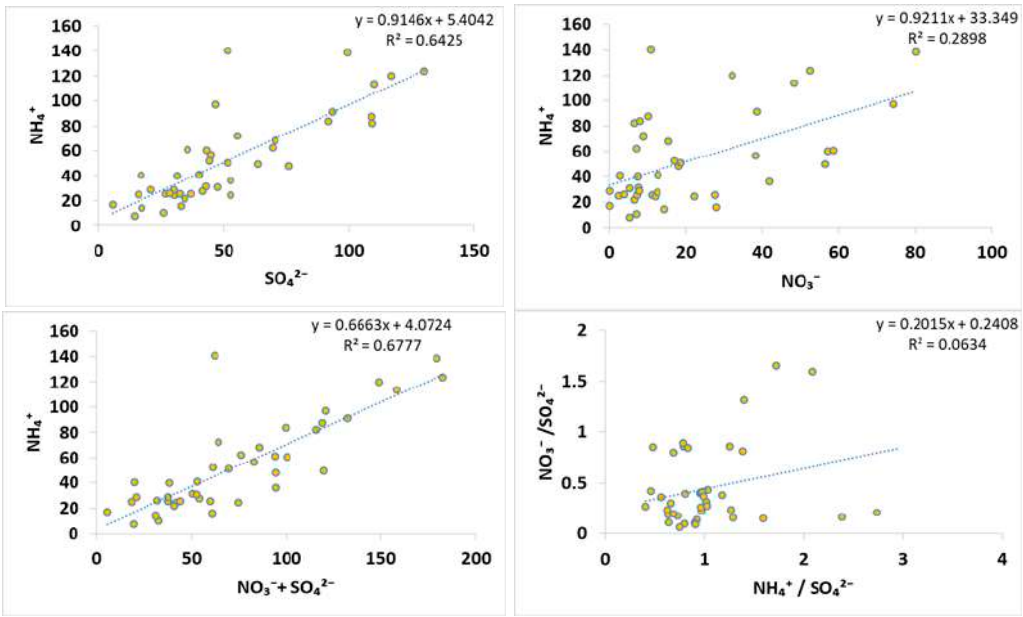

Figure 11. Relationships between SO_4^{2-}, NO_3^-, and NH_4^+ in Mexico City.

3.7. Meteorological Information

Table 2 shows the values of wind speed during the sampling period, with the predominant wind direction from the northwest and north, with the exception of HD in MER when the winds come from the southeast.

Table 2. Meteorological information for UAM and MER.

Season	Relative Humidity (%)	Temperature (°C)	Main Wind Direction	Wind Speed (m/s)	Wind Rose
UAM					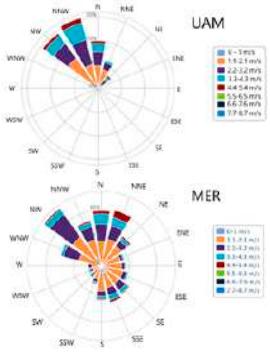
CD	36	15	Northeast	5	
HD	55	26	North	6	
RA	70	17	North	4	
5 January 2022	55.5	11.6	Northwest	0.9	
22 June 2022	45	15	Northeast	5	
MER					
CD	20	18	North	6	
HD	50	25	Southwest	5	
RA	80	15	Northeast	3.7	
19 December 2022	60	12	Northeast	5	
26 September 2022	50	22	Northeast	6	

The primary wind direction showed an influence from the industrial zone, located to the north of the city, affecting mainly UAM and further MER as a receptor site. Secondly, although on a minor scale, the MER site had influences of south and northeast winds several days of the year, modifying the impact from the industrial zone. As was mentioned before, high temperatures favor aerosol production, although UV radiation is the most important variable. The mechanism production of secondary aerosols is related to atmospheric moisture; during RA and CD seasons, RH > 50, meaning that sulfate and nitrate were primarily produced by aqueous-phase SO_2 oxidation, rather than through gas-phase conversion [46].

3.8. Hysplit Backward Trajectories

UAM site backward trajectory analysis was performed for the day with the highest $PM_{2.5}$ concentration (5 January 2022); that day, the air masses were brought to the sampling site from the northwest, passing through large areas of industrial activities to the north of the city. Meanwhile, on the day with the lowest concentration (22 June 2022), the $PM_{2.5}$ masses crossed from the northeast, and despite passing through one of the industrial zones, winds did not pass through both industrial zones, showing, as a consequence, a lower contribution of industrial emissions for that day. A similar effect occurred in MER where on the most polluted day (19 December 2022), the main backward trajectories were from the northwest passing over the industrial zone, whereas on the day with the lowest $PM_{2.5}$ concentration, the air masses arrived from the northwest, while in the UAM and MER.

The highest $PM_{2.5}$ concentrations on the selected days were not only related to the climatological conditions in the CD season but could also be associated with an air mass recirculation phenomenon in the trajectories for both sites. When the air masses circulate around a specific area, they produce resuspension and high pollutant concentrations, favoring bad air quality and possible transport from other sites, as can be seen in Figures 12 and 13. When city conditions do not allow adequate air mass dispersion, this can cause an increase in the concentration [49]; on the opposite side, on the days that presented the lowest concentration, the trajectories continued straight without presenting the recirculation phenomenon.

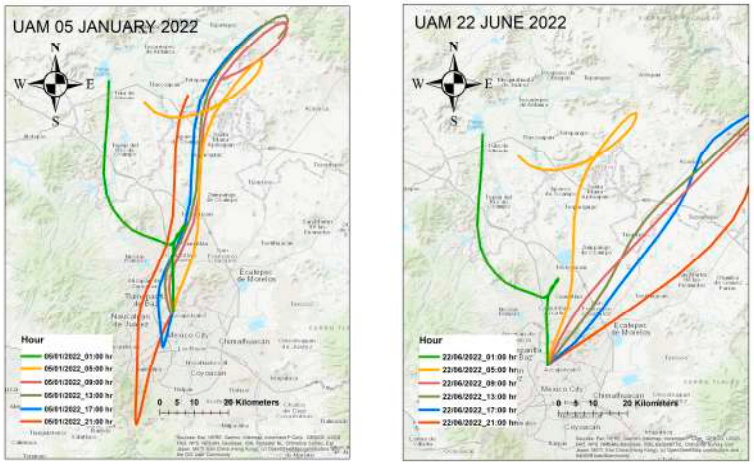

Figure 12. Back trajectories UAM (NOAA Hysplit model). Domain 2000 m; modeled receptor height 20 m.

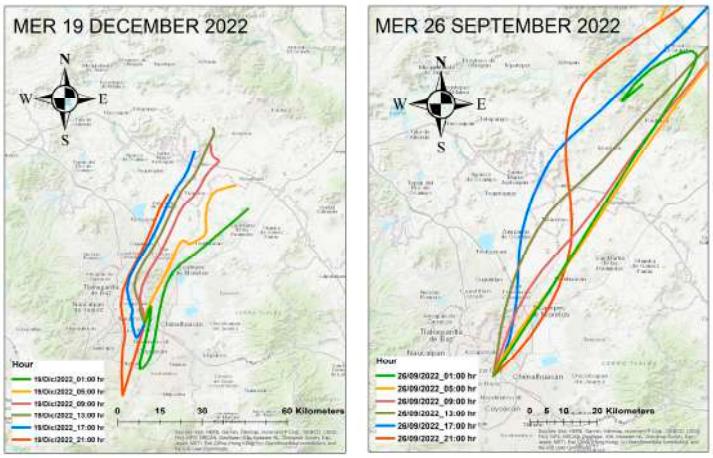

Figure 13. Back trajectories MER (NOAA Hysplit model). Domain 2000 m; modeled receptor height 20 m.

3.9. Positive Matrix Factorization Model

PMF was applied to the 120 data (UAM and MER), where the identified factors corresponded to Factor 1: Vehicular and crustal; Factor 2: secondary aerosols; and Factor 3: industrial and biomass burning. Factor profiles achieved by PMF can include contributions from different sources since they can have similar chemical profiles [23]. In this research, two of the determined factors had mixed sources. Further, the model was applied to each site in order to identify differences between the two locations, obtaining good fit and convergence, despite applying the model with a lesser amount of data, since it is capable of compensating for missing data by achieving the means of the input data. The identified sources were the same, but with different contributions, as can be seen in Table 3 which displays the percentage of each species in the source.

Figure 14 shows the source profiles for each site derived from the PMF model. For the UAM site, Factor 1 had high contributions of NO_2, which is a known tracer of vehicular emissions [50]. NO_3^- and SO_4^{2-} are constituents of vehicular resuspended dust, since a main avenue is close to the site. Moreover, some vehicular emissions control devices have been associated with the NH_3 emissions that could undergo a transformation to secondary NH_4^+ in the vehicular resuspended dust [51]. This first source contributed 54% of $PM_{2.5}$ mass. In Factor 1, crustal is the second source, characterized mainly by specific inorganic ions such as PO_4^{3-}, Na^+, K^+, Ca^{2+}, and Mg^{2+} [14,52] and it contributed 2% of $PM_{2.5}$ mass. The second factor is related also to two sources, one of them being the secondary inorganic

aerosols, accounting for 25% of $PM_{2.5}$ concentration, characterized by high NH_4^+, NO_3^-, and SO_4^{2-} [53–55]; the other source of this factor contributed 1% of $PM_{2.5}$ concentration, and is related to the K^+ that is a biomass-burning tracer with the associated ion Na^+ [56]. Factor 3 contributed 12% of $PM_{2.5}$ mass and is high in Cl^- derived from coal combustion, which plays an important role in this ion's formation, and is used in industrial activities where SO_2 and NO_2 gasses are emitted [14,57].

Table 3. Summary of PMF factors and their specific tracers.

Factor	Site	Source	Tracers
1	Mexico City	VE CR	NO_2, NH_4^+, PO_4^{3-}, Na^+
2	Mexico City	SA	SO_4^{2-}, NH_4^+
3	Mexico City	IN BB	Cl^-, K^+
1	UAM	VE CR	NO_2, NH_4^+, NO_3^-, PO_4^{3-}, Mg^{2+}, Na^+
2	UAM	SA BB	SO_4^{2-}, NO_3^-, NH_4^+, K^+
3	UAM	IN	Cl^-, SO_2, NO_3^-
1	MER	VE IN	NO_2, NH_4^+, Cl^-,
2	MER	SA	SO_4^{2-}, NO_3^-, NH_4^+,
3	MER	CR	Na^+, Mg^{2+}, PO_4^{3-}

(VE) Vehicular, (SA) Secondary Aerosols, (IN) Industrial, (CR) Crustal, (BB) Biomass burning.

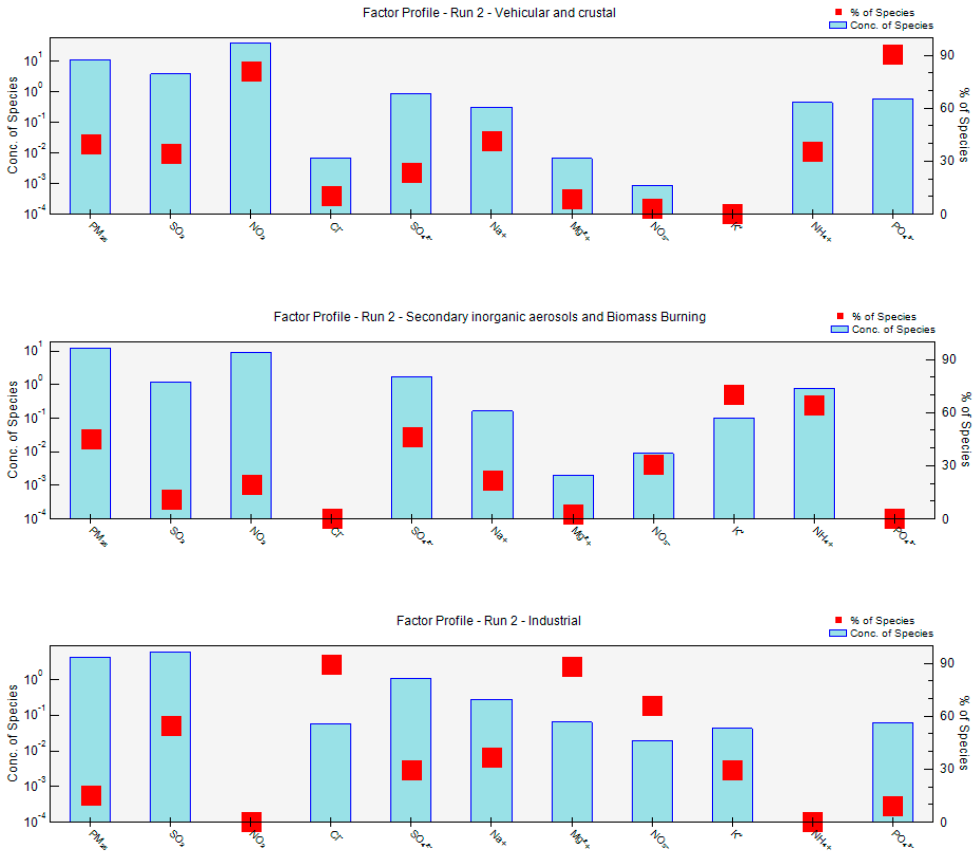

Figure 14. $PM_{2.5}$ source profiles in UAM from December 2021 to December 2022.

The second Factor was able to determine the two same sources identified in UAM, secondary aerosols related to the high presence of NO_3^-, SO_4^{2-}, and NH_4^+ ions, accounting for 20% of particle mass [58,59], and the biomass burning identified by the presence of K^+, with a contribution of <2%. The third Factor was associated with crustal dust due to high Na^+, Mg^{2+}, and low PO_4^{3-} (Figure 15).

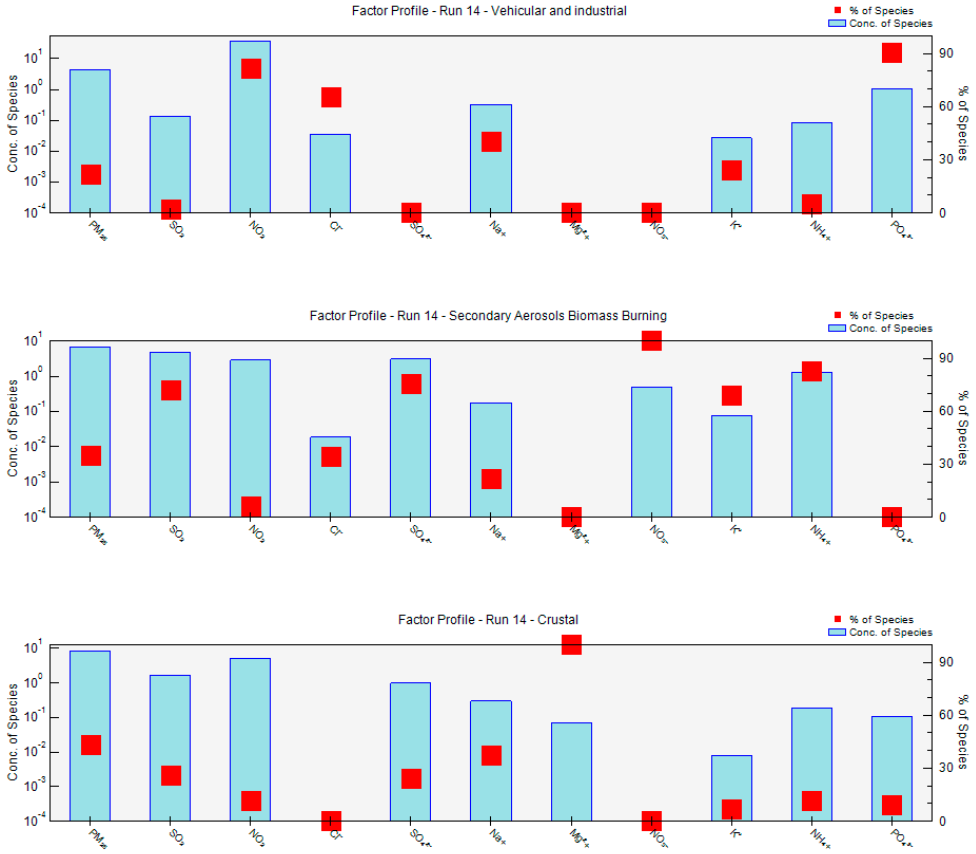

Figure 15. $PM_{2.5}$ source profiles in MER from December 2021 to December 2022 period.

The summary of the sources found with the PMF model is presented in Figure 16. Vehicular resuspended dust and emissions were the highest contributors to UAM and MER with 57.5% and 50%, respectively, since sites are located close to main avenues. The accounting of secondary aerosols was practically identical in both sites, showing that there were similar mixtures of their precursor gases in the two zones. The larger apportionment of the crustal source in MER is attributed to the construction work near the area, and the influence of the industrial zones in MER is evident, with a contribution of around 13% versus 3% in MER. The biomass burning had a minimal contribution in UAM.

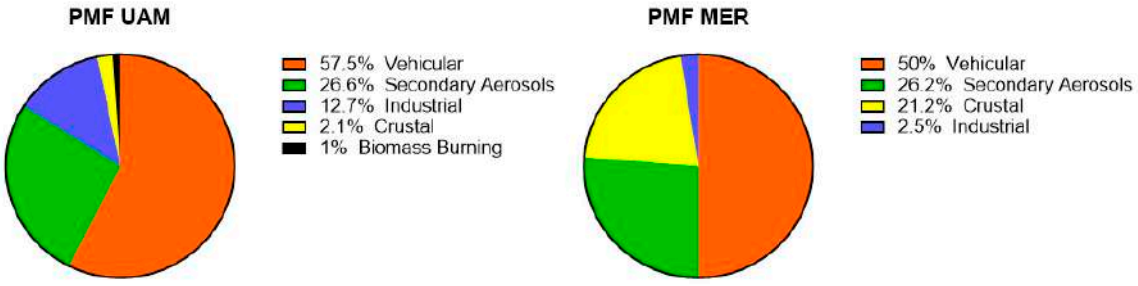

Figure 16. Source contribution by site, December 2021–December 2022 period.

The comparison of WSII concentrations and their source apportionment in this research, compared to other urban sites, is shown in Table 4. With the exception of Tetuan in Morocco, Mexico City presented the lowest $PM_{2.5}$ and WSII concentrations among the cities due to different sources and industrialization.

Table 4. Comparison of water-soluble ion concentrations in $PM_{2.5}$ in $\mu g/m^3$ and in associated sources determined using the PMF model.

Parameter	Mexico City (This Study)	Tetuan Morocco [54]	Jiangsu China [60]	Wuhan China [61]	Nanjing China [62]	Lyliang China [51]	Lanzhou China [63]
$\mu g/m^3$							
$PM_{2.5}$	24	18	68.9	101.3	91.2	36.3	54.3
ΣWSII	10.7	6	32.4	59	44.9	29.1	13.2
SO_4^{2-}	4.5	3	9.0	18.9	23.2	7.6	3.9
NO_3^-	1.8	1.1	10.5	13.7	16.9	8.8	3.3
NH_4^+	1.6	1	6.4	24.9	5.3	7.3	1.3
K^+	0.2	ND	0.9	0.1	1.6	ND	0.4
Cl^-	0.1	ND	1.7	0.8	2.1	4.7	2.6
%							
$SNA/PM_{2.5}$	32.9	28.3	37.6	56.8	49.8	65.3	15.7
Secondary Aerosols/$PM_{2.5}$	26.4	ND	20	35	27	43	10.8
Sources	VE, SA, IN, CR, BB	AM, RT, BB, FSEA, ASEA, ORF	VE, BB, SA, DU	RD, SEA, SN, SAM, CC, BB	DU, SS, INMS, BB	SA, BB, CC, DU, VE	DU, IN, BB, MES, SA, SES

(VE) Vehicular; (SA) Secondary Aerosols; (IN) Industrial; (CR) Crustal; (BB) Biomass Burning; (DU) Dust; (AM) Ammonium Sulfate; (RT) Road Traffic; (FSEA) Fresh sea salt; (ASEA) Aged sea salt; (SES) Sea spray; (CC) Coal Combustion; (RD) Road dust; (SN) Secondary nitrate; (SS) Secondary sulfate; (MES) Metal smelting. SNA: sum of sulfate, nitrate, and ammonium. ND: Not determined.

SO_4^{2-}, NH_4^+, and NO_3^- (SNA) accounted for 32.9%, on average, of the total $PM_{2.5}$ mass in Mexico City sites, which is similar to SNA measured in Jiangsu, China [60], and Tetuan in Morocco [54], but lower than in Wuhan [61], Nanjing [62], and Lyliang [51], which are Chinese industrial cities. On the opposite hand, this study recorded SNA concentrations two times higher than in the study performed during the spring in Lanzhou [63] where 17% of monitoring days presented dust storms, increasing crustal ions with the decrease in NO_3^- and NH_4^+ levels.

Regarding the contribution of secondary aerosol to $PM_{2.5}$ total mass, this study shows similar percentages to most Chinese cities, with the exception of Lanzhou in the storm season and Lyliang, where secondary aerosol contribution is too high (43%) due to great industrialization, ranking first, third, and fourth for soot, sulfur dioxide, and industrial dust emissions, respectively, in China [63].

4. Conclusions

This research reports the water soluble inorganic ion (WSII) characterization in $PM_{2.5}$ as well as the ion source apportionment in two sites in Mexico City over one year. The annual average $PM_{2.5}$ concentrations at the Metropolitan Autonomous University and Merced were 28.4 ± 11.1 $\mu g\ m^{-3}$ and 20.7 ± 8.3 $\mu g\ m^{-3}$, respectively, both exceeding the OMS air quality guidelines. Seasonal variations in $PM_{2.5}$ and WSII were CD > HD > RA in both sites, due mainly to weather conditions and impacts from industrial zones. Water-soluble inorganic ions had contributions between 40 and 50% of $PM_{2.5}$ total mass, and SO_4^{2-}, NH_4^+, and NO_3^- (SNA) concentrations were the most abundant ions, representing 50–70% of the total ions; these concentrations are lower than those reported in Chinese industrialized cities. Differences between the two sites are due to differences in sources, weather, and impacts from industrial zones, as was shown by wind roses and source apportionment by the PMF model. The CE/AE ratios for UAM and MER were lower than one, indicating $PM_{2.5}$ acidity, which was confirmed with direct pH measurements. This acidity is a characteristic of the Mexico City atmosphere, which is different to other cities in China with excess alkaline ions in their atmosphere. This is confirmed by the relationships among the SNA ions, showing a poor ammonium atmosphere with low NH_4NO_3 formation. Moreover, the NOR median annual values for UAM and MER were 0.01 ± 0.02 and 0.02 ± 0.009, respectively, showing the lowest levels in the hot dry season

where high temperatures can evaporate the formed nitrate secondary aerosol. On the contrary, SOR values were 0.21 ± 0.06 and 0.28 ± 0.03, respectively, indicating the high production of sulfate secondary aerosols because high solar radiation during the whole year in Mexico City promotes the SO_2 photochemical transformation to sulfate secondary aerosol. Backward trajectories with the Hysplit model performed at 20 m demonstrated that during the most polluted days, a recirculation phenomenon of winds was presented, raising the dust resuspension and accumulation of pollutants. WSII source apportionment in 2022 was comprehensively analyzed applying the PMF model, meaning that their major sources were the vehicular emissions and resuspended dust, followed by secondary aerosols in both sites. But, in MER, the third source was crustal dust, whereas in UAM it was the industrial emissions. These results are useful for policy makers since they provide evidence for carrying out inspections of industrial emissions and for tightening sulfur and nitrogen dioxide emission standards, which not only impact the closest areas, but also more remote receiving sites.

Author Contributions: Conceptualization: F.M.-V. and V.M.-Á.; Methodology: R.S.-E. and A.L.A.-J.; Formal Analysis: J.d.J.F.-L.; Software: F.M.-V.; Validation: B.L.V.-H.; Writing review and revision: M.T.-R.; Project administration and funding acquisition. All authors have read and agreed to the published version of the manuscript.

Funding: CONAHCyT project 316644.

Data Availability Statement: Data could be shared as request.

Acknowledgments: This research was supported by the 316642 CONAHCyT project. The authors thank the personnel of SCA-ICA y CC UNAM, Mónica Solano Murillo, for her help in analysis; to the UAM-A Basic Sciences department for the support; and the NOAA Air Resources Laboratory is acknowledged for provision of the HYSPLIT model and the READY website used in this research. F. Millán acknowledges a graduate scholarship from CONAHCYT.

Conflicts of Interest: The authors declare no conflict of interest.

References

1. World Health Organization (WHO). WHO Global Guidelines on Air Quality: Suspended Particles (PM2.5 and PM10), Ozone, Nitrogen Dioxide, Sulfur Dioxide and Carbon Monoxide. Summary [WHO Global Air Quality Guidelines: Particulate Matter (PM2.5 and PM10), Ozone, Nitrogen Dioxide, Sulfur Dioxide and Carbon Monoxide 2021. Available online: https://www.who.int/publications/i/item/9789240034228 (accessed on 15 October 2023).
2. Maya, A.; Del Pilar, M.; Posada, P.I.M.; Nowak, D.J.; Hoehn, R.E. Remoción de contaminantes atmosféricos por el bosque urbano en el valle de Aburrá. *Colomb. For.* **2019**, *22*, 5–16. [CrossRef]
3. Correa, M.A.; Franco, S.A.; Gómez, L.M.; Aguiar, D.; Colorado, H.A. Characterization Methods of Ions and Metals in Partic-ulate Matter Pollutants on PM2.5 and PM10 Samples from Several Emission Sources. *Sustainability* **2023**, *15*, 4402. [CrossRef]
4. Wang, D.; Qu, W.J.; Cao, G.L.; Zhang, X.Y.; Che, H.Z. (Analysis of water-soluble species in emission particulate from regional stalk burning and their emission factors). *China Powder Sci. Technol.* **2008**, *29*, 305–309.
5. Parrish, D.D.; Kuster, W.C.; Shao, M.; Yokouchi, Y.; Kondo, Y.; Goldan, P.D.; de Gouw, J.A.; Koike, M.; Shirai, T. Comparison of air pollutant emissions among mega-cities. *Atmos. Environ.* **2009**, *43*, 6435–6441. [CrossRef]
6. Mugica, V.; Ortiz, E.; Molina, L.; De Vizcaya-Ruiz, A.; Nebot, A.; Quintana, R.; Aguilar, J.; Alcántara, E. PM Composition and Source Reconciliation in Mexico City. *Atmos. Environ.* **2009**, *43*, 5068–5074.
7. Molina, L.; Molina, M.J. (Eds.) *Air Quality in the Mexico Megacity: An Integrated Assessment*; Springer Science & Business Media: Berlin/Heidelberg, Germany, 2002; Volume 2.
8. WHO. Air Quality Deteriorating in Many of the World's Cities. Available online: https://www.who.int/news/item/07-05-2014-air-quality-deteriorating-in-many-of-the-world-s-cities (accessed on 30 September 2023).
9. IPCC, Climate Change. The Physical Science Basis. In *Contribution of Working Group I to the Fourth Assessment Report of the Intergovernmental Panel on Climate Change*; Solomon, S., Qin, D., Manning, M., Chen, Z., Marquis, M., Averyt, K.B., Tignor, M., Miller, H.L., Eds.; Cambridge University Press: Cambridge, UK; New York, NY, USA, 2007; p. 996.
10. Zhang, L.; Vet, R.; Wiebe, A.; Mihele, C.; Sukloff, B.; Chan, E.; Moran, M.D.; Iqbal, S. Characterization of the size-segregated water-soluble inorganic ions at eight Canadian rural sites. *Atmos. Meas. Tech.* **2008**, *8*, 7133–7151. [CrossRef]
11. Zhang, T.; Cao, J.J.; Tie, X.X.; Shen, Z.X.; Liu, S.X.; Ding, H.; Li, W.T. Water-soluble ions in atmospheric aerosols measured in Xi'an, China: Seasonal variations and sources. *Atmos. Res.* **2011**, *102*, 110–119. [CrossRef]
12. Salam, A.; Assaduzzaman; Hossain, M.N.; Alam Siddiki, A.K.M.N. Water Soluble Ionic Species in the Atmospheric Fine Particulate Matters ($PM_{2.5}$) in a Southeast Asian Mega City (Dhaka, Bangladesh). *Open J. Air Pollut.* **2015**, *4*, 99–108. [CrossRef]

13. Rogula-Kozłowska, W.; Błaszczak, B.; Szopa, S.; Klejnowski, K.; Sówka, I.; Zwoździak, A.; Jabłońska, M.; Mathews, B. $PM_{2.5}$ in the central part of Upper Silesia, Poland: Concentrations, elemental composition, and mobility of components. *Environ. Monit. Assess.* **2013**, *185*, 581–601. [CrossRef]
14. Liu, Z.; Xie, Y.; Hu, B.; Wen, T.; Xin, J.; Li, X.; Wang, Y. Size-resolved aerosol water-soluble ions during the summer and winter seasons in Beijing: Formation mechanisms of secondary inorganic aerosols. *Chemosphere* **2017**, *183*, 119–131. [CrossRef]
15. Farren, N.J.; Dunmore, R.E.; Mead, M.I.; Nadzir, M.S.M.; Abu Samah, A.; Phang, S.-M.; Bandy, B.J.; Sturges, W.T.; Hamilton, J.F. Chemical characterisation of water-soluble ions in atmospheric particulate matter on the east coast of Peninsular Malaysia. *Atmos. Meas. Tech.* **2019**, *19*, 1537–1553. [CrossRef]
16. He, Q.; Yan, Y.; Guo, L.; Zhang, Y.; Zhang, G.; Wang, X. Characterization and source analysis of water-soluble inorganic ionic species in $PM_{2.5}$ in Taiyuan city, China. *Atmos. Res.* **2017**, *184*, 48–55. [CrossRef]
17. Han, L.; Cheng, S.; Zhuang, G.; Ning, H.; Wang, H.; Wei, W.; Zhao, X. The changes and long-range transport of $PM_{2.5}$ in Beijing in the past decade. *Atmos. Environ.* **2015**, *110*, 186–195. [CrossRef]
18. Berner, E.K. *Acid Rain and Acid Deposition*; Salem Press Encyclopedia of Science; Grey House Publishing: Amenia, NY, USA, 2013.
19. Zhang, Y.; Tang, A.; Wang, C.; Ma, X.; Li, Y.; Xu, W.; Xia, X.; Zheng, A.; Li, W.; Fang, Z.; et al. $PM_{2.5}$ and water-soluble inorganic ion concentrations decreased faster in urban than rural areas in China. *J. Environ. Sci.* **2022**, *122*, 83–91. [CrossRef] [PubMed]
20. Sun, Y.-C.; Jiang, N.; Wang, S.-B.; Duan, S.-G.; Zahng, R.-Q. Seasonal Characteristics and Source Analysis of Water-Soluble Ions in $PM_{2.5}$ of Anyang City. *Huan Jing Ke Xue* **2020**, *41*, 75–81.
21. Salam, A.; Bauer, H.; Kassin, K.; Ullah, S.M.; Puxbaum, H. Aerosol Chemical Characteristics of a MegaCity in Southeast Asia (Dhaka, Bangladesh). *Atmos. Environ.* **2003**, *37*, 2517–2528. [CrossRef]
22. Rolph, G.D.; Ngan, F.; Draxler, R.R. Modeling the fallout from stabilized nuclear clouds using the HYSPLIT atmospheric dis-persion model. *J. Environ. Radioact.* **2014**, *136*, 41–55.5. [CrossRef]
23. Cesari, D.; Donateo, A.; Conte, M.; Merico, E.; Giangreco, A.; Giangreco, F.; Contini, D. An inter-comparison of $PM_{2.5}$ at urban and urban background sites: Chemical characterization and source apportionment. *Atmos. Res.* **2016**, *174*, 106–119. [CrossRef]
24. Belis, C.; Karagulian, F.; Amato, F.; Almeida, M.; Artaxo, P.; Beddows, D.; Bernardoni, V.; Bove, M.; Carbone, S.; Cesari, D.; et al. A new methodology to assess the performance and uncertainty of source apportionment models II: The results of two European intercomparison exercises. *Atmos. Environ.* **2015**, *123*, 240–250. [CrossRef]
25. Meng, C.; Wang, L.; Zhang, F.; Wei, Z.; Ma, S.; Ma, X.; Yang, J. Characteristics of concentrations and water-soluble inorganic ions in $PM_{2.5}$ in Handan City, Hebei province, China. *Atmos. Res.* **2016**, *171*, 133–146. [CrossRef]
26. Yin, L.; Niu, Z.; Chen, X.; Chen, J.; Zhang, F.; Xu, L. Characteristics of water-soluble inorganic ions in $PM_{2.5}$ and $PM_{2.5-10}$ in the coastal urban agglomeration along the Western Taiwan Strait Region, China. *Environ. Sci. Pollut. Res.* **2014**, *21*, 5141–5156. [CrossRef] [PubMed]
27. Chow, J.C.; Fujita, E.M.; Watson, J.G.; Lu, Z.; Lawson, D.R.; Ashbaugh, L.L. Evaluation of filter-based aerosol measurements during the 1987 Southern California Air Quality Study. *Environ. Monit. Assess.* **1994**, *30*, 49–80. [CrossRef] [PubMed]
28. Li, T.-C.; Yuan, C.-S.; Huang, H.-C.; Lee, C.-L.; Wu, S.-P.; Tong, C. Inter-comparison of seasonal variation, chemical characteristics, and source identification of atmospheric fine particles on both sides of the Taiwan strait. *Sci. Rep.* **2016**, *6*, 22956. [CrossRef] [PubMed]
29. Xu, J.; Song, S.; Harrison, R.M.; Song, C.; Wei, L.; Zhang, Q.; Sun, Y.; Lei, L.; Zhang, C.; Yao, X.; et al. An interlaboratory comparison of aerosol inorganic ion measurements by ion chromatography: Implications for aerosol pH estimate. *Atmos. Meas. Tech.* **2020**, *13*, 6325–6341. [CrossRef]
30. Zheng, H.; Kong, S.; Yan, Q.; Wu, F.; Cheng, Y.; Zheng, S.; Wu, J.; Yang, G.; Zheng, M.; Tang, L.; et al. The impacts of pollution control measures on $PM_{2.5}$ reduction: Insights of chemical composition, source variation and health risk. *Atmos. Environ.* **2018**, *197*, 103–117. [CrossRef]
31. Hernández-Moreno, A.; Trujillo-Páez, F.I.; Mugica-Álvarez, V. Quantification of primary $PM_{2.5}$ Mass Exchange in three Mexican Megalopolis Metropolitan Areas. *Urban Clim.* **2023**, *51*, 101608. [CrossRef]
32. Nan, J.; Ke, W.; Xue, Y.; Fangcheng, S.; Shasha, Y.; Qiang, L.; Ruiqin, Z. Chemical Characteristics and Source Apportionment by Two Receptor Models of Size-segregated Aerosols in an Emerging Megacity in China. *Aerosol Air Qual.* **2018**, *18*, 1375–1390.
33. Wang, Y.Q. MeteoInfo: GIS software for meteorological data visualization and analysis. *Meteorol. Appl.* **2014**, *21*, 360–368. [CrossRef]
34. Xie, Y.; Lu, H.; Yi, A.; Zhang, Z.; Zheng, N.; Fang, X.; Xiao, H. Characterization and source analysis of water–soluble ions in $PM_{2.5}$ at a background site in Central China. *Atmos. Res.* **2020**, *239*, 104881. [CrossRef]
35. Hernández-López, A.E.; del Campo, J.M.M.; Mugica-Álvarez, V.; Hernández-Valle, B.L.; Mejía-Ponce, L.V.; Pineda-Santamaría, J.C.; Reynoso-Cruces, S.; Mendoza-Flores, J.A.; Rozanes-Valenzuela, D. A study of $PM_{2.5}$ elemental composition in southwest mexico city and development of receptor models with positive matrix factorization. *Rev. Int. De Contam. Ambient.* **2020**, *37*, 67–88. [CrossRef]
36. Shen, Z.; Cao, J.; Arimoto, R.; Han, Y.; Zhu, C.; Tian, J.; Liu, S. Chemical Characteristics of Fine Particles (PM_1) from Xi'an, China. *Aerosol Sci. Technol.* **2010**, *44*, 461–472. [CrossRef]
37. Li, Q.; Jiang, N.; Yu, X.; Dong, Z.; Duan, S.; Zhang, L.; Zhang, R. Sources and spatial distribution of $PM_{2.5}$-bound polycyclic aromatic hydrocarbons in Zhengzhou. *Atmos. Res.* **2016**, *216*, 65–75. [CrossRef]

38. Jang, E.; Alam, M.S.; Harrison, R.M. Source apportionment of polycyclic aromatic hydrocarbons in urban air using positive matrix factorization and spatial distribution analysis. *Atmos. Environ.* **2013**, *79*, 271–285. [CrossRef]
39. Allan, M.A. *Manual for the GAW Precipitation Chemistry Program: Guidelines, Data Quality Objectives and Standard Operating Procedures*; World Meteorological Organization: Geneva, Switzerland, 2004.
40. Tian, S.; Pan, Y.; Wang, Y. Ion balance and acidity of size-segregated particles during haze episodes in urban Beijing. *Atmos. Res.* **2018**, *201*, 159–167. [CrossRef]
41. Guo, Q.; Chen, K.; Xu, G. Characteristics and Sources of Water-Soluble Inorganic Ions in $PM_{2.5}$ in Urban Nanjing, China. *Atmosphere* **2023**, *14*, 135. [CrossRef]
42. Geng, N.; Wang, J.; Xu, Y. $PM_{2.5}$ in an industrial district of Zhengzhou, China: Chemical composition and source 309 apportionment. *Particuology* **2013**, *11*, 99–109. [CrossRef]
43. Budhavant, K.B.; Rao, P.S.P.; Safai, P.D.; Gawhane, R.D.; Raju, M.P. Chemistry of rainwater and aerosols over Bay of Bengal during CTCZ program. *J. Atmos. Chem.* **2010**, *65*, 171–183. [CrossRef]
44. Xiong, C.; Yu, S.; Chen, X.; Li, Z.; Zhang, Y.; Li, M.; Liu, W.; Li, P.; Seinfeld, J.H. Dominant Contributions of Secondary Aerosols and Vehicle Emissions to Water-Soluble Inorganic Ions of $PM_{2.5}$ in an Urban Site in the Metropolitan Hangzhou, China. *Atmosphere* **2021**, *12*, 1529. [CrossRef]
45. Sitaras, I.E.; Siskos, P.A. The role of primary and secondary air pollutants in atmospheric pollution: Athens urban area as a case study. *Environ. Chem. Lett.* **2008**, *6*, 59–69. [CrossRef]
46. Zhang, R.; Sun, X.; Shi, A.; Huang, Y.; Yan, J.; Nie, T.; Yan, X.; Li, X. Secondary inorganic aerosols formation during haze episodes at an urban site in Beijing, China. *Atmos. Environ.* **2018**, *177*, 275–282. [CrossRef]
47. Yao, X.; Chan, C.K.; Fang, M.; Cadle, S.; Chan, T.; Mulawa, P.; He, K.; Ye, B. The water-soluble ionic composition of PM2.5 in Shanghai and Beijing, China. *Atmos. Environ.* **2002**, *36*, 4223–4234. [CrossRef]
48. Suzuki, I.; Hayashi, K.; Igarashi, Y.; Takahashi, H.; Sawa, Y.; Ogura, N.; Akagi, T.; Dokiya, Y. Seasonal variation of water-soluble ion species in the atmospheric aerosols at the summit of Mt. Fuji. *Atmos. Environ.* **2008**, *42*, 8027–8035. [CrossRef]
49. IBC-CSIC. Estudio de Evaluación Preliminar de Niveles de Hidrocarburos Aromáticos Policiclicos (PAHs) en Aire Ambiente en la Comunidad Autónoma de Aragon Durante el Periodo Estival. *DGA-Dpto. Medio Ambiente.* **2009**, 17–35. Available online: http://docplayer.es/148271981-Estudio-de-evaluacion-preliminar-de-niveles-de-hidrocarburos-aromaticos-policiclicos.html (accessed on 10 October 2023).
50. Alvarado, A.S.; Luján, P.M.; Bomblat, C. Modelación de las emisiones del parque automotor en la ciudad de Cochabam-ba-Bolivia. *Acta Nova* **2004**, *2*, 475–492.
51. Liu, T.; Mu, L.; Li, X.; Li, Y.; Liu, Z.; Jiang, X.; Feng, C.; Zheng, L. Characteristics and source apportionment of water-soluble inorganic ions in atmospheric particles in Lvliang, China. *Environ. Geochem. Health* **2023**, *45*, 4203–4217. [CrossRef]
52. Kim, S.; Kim, T.-Y.; Yi, S.-M.; Heo, J. Source apportionment of $PM_{2.5}$ using positive matrix factorization (PMF) at a rural site in Korea. *J. Environ. Manag.* **2018**, *214*, 325–334. [CrossRef]
53. Cui, Y.; Yin, Y.; Chen, K.; Zhang, X.; Kuang, X.; Jiang, H.; Wang, H.; Zhen, Z.; He, C. Characteristics and sources of WSI in North China Plain: A simultaneous measurement at the summit and foot of Mount Tai. *J. Environ. Sci.* **2020**, *92*, 264–277. [CrossRef]
54. Benchrif, A.; Guinot, B.; Bounakhla, M.; Cachier, H.; Damnati, B.; Baghdad, B. Aerosols in Northern Morocco: Input pathways and their chemical fingerprint. *Atmos. Environ.* **2018**, *174*, 140–147. [CrossRef]
55. Zhang, R.; Jing, J.; Tao, J.; Hsu, S.-C.; Wang, G.; Cao, J.; Lee, C.S.L.; Zhu, L.; Chen, Z.; Zhao, Y.; et al. Chemical characterization and source apportionment of $PM_{2.5}$ in Beijing: Seasonal perspective. *Atmos. Chem. Phys.* **2013**, *13*, 7053–7074. [CrossRef]
56. Chen, Y.-C.; Shie, R.-H.; Zhu, J.-J.; Hsu, C.-Y. A hybrid methodology to quantitatively identify inorganic aerosol of $PM_{2.5}$ source contribution. *J. Hazard. Mater.* **2022**, *428*, 128173. [CrossRef] [PubMed]
57. He, J. Pollution haven hypothesis and environmental impacts of foreign direct investment: The case of industrial emission of sulfur dioxide (SO_2) in Chinese provinces. *Ecol. Econ.* **2006**, *60*, 228–245. [CrossRef]
58. Bi, X.; Dai, Q.; Wu, J.; Zhang, Q.; Zhang, W.; Luo, R.; Cheng, Y.; Zhang, J.; Wang, L.; Yu, Z.; et al. Characteristics of the main primary source profiles of particulate matter across China from 1987 to 2017. *Atmos. Meas. Tech.* **2019**, *19*, 3223–3243. [CrossRef]
59. Dai, L.; Wang, L.; Li, L.; Liang, T.; Zhang, Y.; Ma, C.; Xing, B. Multivariate geostatistical analysis and source identification of heavy metals in the sediment of Poyang Lake in China. *Sci. Total. Environ.* **2018**, *621*, 1433–1444. [CrossRef]
60. Cui, Y.; Zhu, L.; Wang, H.; Zhao, Z.; Ma, S.; Ye, Z. Characteristics and Oxidative Potential of Ambient $PM_{2.5}$ in the Yangtze River Delta Region: Pollution Level and Source Apportionment. *Atmosphere* **2023**, *14*, 425. [CrossRef]
61. Ding, L.; Fang, X.; Dong, H.; Zhao, W. Characteristics of $PM_{2.5}$ water-soluble ions and source identification during springtime 2017 in Wuhan. *Ekoloji* **2019**, *28*, 505–515.
62. Gong, J.; Tao, M.; Liu, Q.; Ding, C.; Li, P.; Schauer, J.J. Sources of Aerosol Acidity at a Suburban Site of Nanjing and Their Associations with Chlorophyll Depletion. *ACS Earth Space Chem.* **2021**, *5*, 3437–3447. [CrossRef]
63. Cheng, B.; Ma, Y.; Li, H.; Feng, F.; Zhang, Y.; Qin, P. Water-soluble ions and source apportionment of $PM_{2.5}$ depending on synoptic weather patterns in an urban environment in spring dust season. *Sci. Rep.* **2022**, *12*, 21953. [CrossRef] [PubMed]